

M-LRM: Multi-view Large Reconstruction Model

Mengfei Li¹, Xiaoxiao Long^{1✉}, Yixun Liang³, Weiyu Li¹, Yuan Liu², Peng Li¹
 Xiaowei Chi¹, Xingqun Qi¹, Wei Xue¹, Wenhan Luo¹, Qifeng Liu^{1✉}, Yike Guo¹
¹HKUST ²HKU ³HKUST(GZ)

mengfei.li@connect.ust.hk, xxlong@connect.hku.hk, liuqifeng@ust.hk

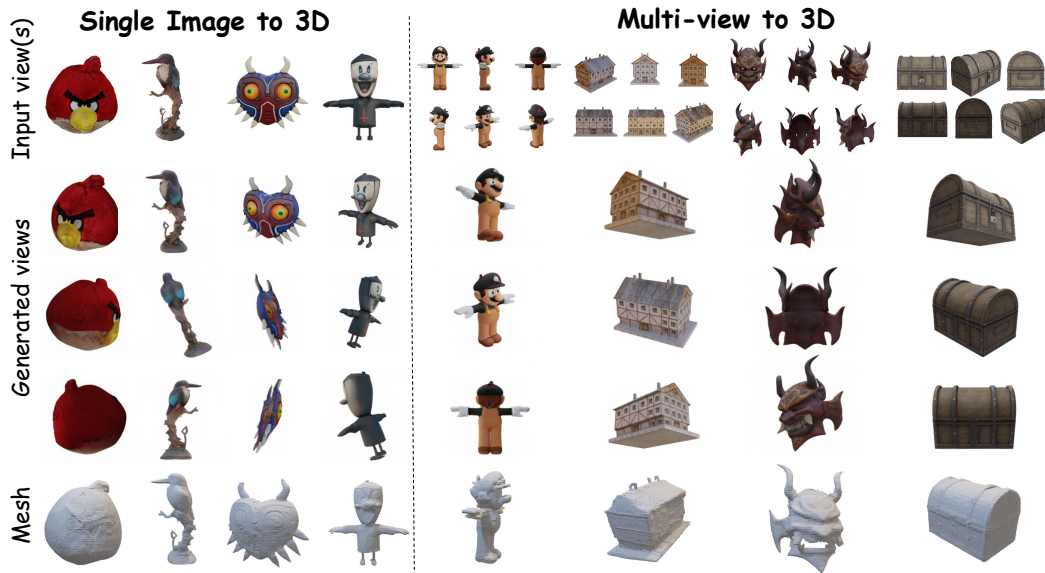


Figure 1: Our M-LRM can generate novel views of high fidelity and meshes of high quality given single or multiple views as input.

Abstract

Despite recent advancements in the Large Reconstruction Model (LRM) demonstrating impressive results, when extending its input from single image to multiple images, it exhibits inefficiencies, subpar geometric and texture quality, as well as slower convergence speed than expected. It is attributed to that, LRM formulates 3D reconstruction as a naive images-to-3D translation problem, ignoring the strong 3D coherence among the input images. In this paper, we propose a Multi-view Large Reconstruction Model (M-LRM) designed to efficiently reconstruct high-quality 3D shapes from multi-views in a 3D-aware manner. Specifically, we introduce a multi-view consistent cross-attention scheme to enable M-LRM to accurately query information from the input images. Moreover, we employ the 3D priors of the input multi-view images to initialize the tri-plane tokens. Compared to LRM, the proposed M-LRM can produce a tri-plane NeRF with 128×128 resolution and generate 3D shapes of high fidelity. Experimental studies demonstrate that our model achieves a significant performance gain and faster training convergence than LRM. Project page: <https://murphy1mf.github.io/M-LRM/>

✉ Corresponding authors.

1 Introduction

3D reconstruction from multi-view images stands as a fundamental and critical task that has garnered decades of study, playing a pivotal role in various downstream applications including virtual reality, 3D content generation, and robotic grasping. Achieving complete and high-quality reconstructions typically necessitates capturing images from dense viewpoints that offer comprehensive coverage of the target object. However, traditional approaches relying on dense viewpoint images face significant degradation when confronted with limited inputs, such as few or even single images. This limitation results in distorted and incomplete reconstructions due to the inadequacy of information provided. Despite attempts to address 3D reconstruction from a few images or even a single image, existing methods often suffer from inefficiency or yield low-quality results.

Recently, the introduction of the Large Reconstruction Model (LRM) and its multi-view variant, Instant3D, has demonstrated remarkable results, indicating the feasibility of learning a generic 3D prior for reconstructing objects from single images or limited image sets. However, LRM approaches the task of 3D reconstruction from images by simplistically treating it as an image-to-3D regression problem. This involves directly training a highly scalable transformer on extensive data to learn the image-to-3D mapping. Regardless of whether a single image or multiple images are provided as input, LRM first unpacks feature maps of the input images into tokens and then feeds the tokens into the transformer to inherently learn 3D priors. Consequently, when extending the input from a single image to multiple images, the LRM model fails to exhibit significant performance improvements since it disregards the 3D coherence among the input images.

In this paper, we introduce a novel architecture designed for reconstructing 3D shapes from multiple images in a 3D-aware manner, termed as the Multi-view Large Reconstruction Model (M-LRM). In contrast to the LRM, which primarily relies on regressing 3D shapes from images without considering their interrelations, our model draws inspiration from traditional Multi-view Stereo (MVS) techniques and explicitly learns correspondences among input images to infer the 3D geometry. Our model builds upon the triplane-based transformer architecture introduced by LRM, leveraging its scalability on extensive datasets. Specifically, we propose a new multi-view consistent cross-attention scheme, which empowers M-LRM to infer 3D geometry by meticulously examining semantic consistency across input images. Furthermore, we introduce a geometry-aware positional embedding approach that directly incorporates the 3D information encoded in multiple images into the transformer architecture. These two innovations enable M-LRM to learn 3D representations from images in a 3D-aware manner, thereby producing high-quality geometries.

Extensive experiments demonstrate that our M-LRM can generate high-quality 3D objects. It is capable of producing accurate views and geometry. Additionally, our experiments show that incorporating explicit 3D priors into the LRM model significantly speeds up convergence. In summary, our key contributions are as follows:

- Our M-LRM addresses the shortcomings of instant3D, which lacks modeling of spatial correlation among multiple input views. This leads to slow convergence and sub-optimal generation results. Instead, our M-LRM leverages the spatial coherence of input images to efficiently generate high-fidelity results.
- We propose a novel Geometry-aware Positional Embedding mechanism to fully utilize image prior. This helps the randomly initialized tri-plane capture spatial and image priors, enabling faster convergence of our M-LRM.
- We introduce a multi-view consistent cross-attention scheme to accurately query information from relevant image regions. This incorporates explicit spatial priors, making the 3D generative model geometry aware. As a result, our M-LRM can generate consistent novel views and high-quality geometry.
- Through extensive experiments, we demonstrate that our M-LRM outperforms all baseline methods in sparse-view reconstruction tasks. It can also generate high-quality 3D objects with a single image input when equipped with a multi-view generation model like Zero123++ [49].

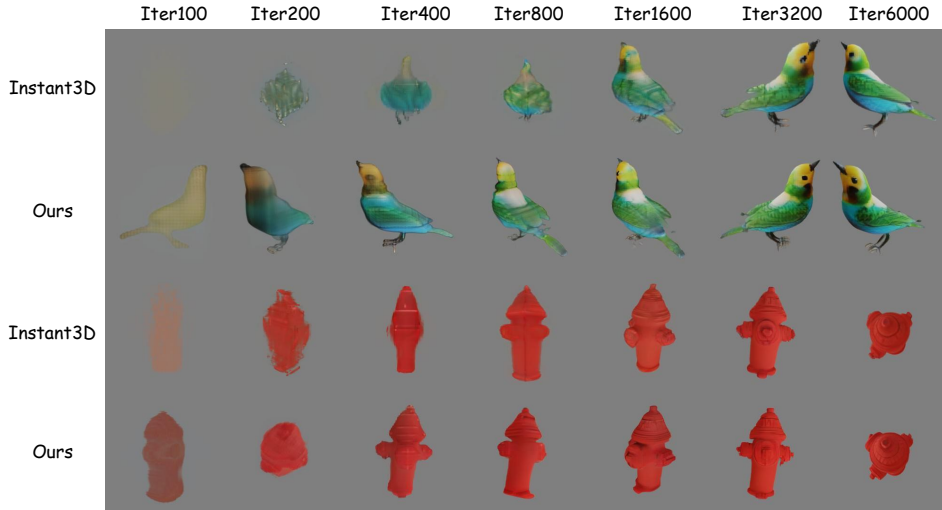


Figure 2: **Visualization of intermediate results during training process.** Compared with existing LRM-based approaches, like Instant3D [29], our proposed GCA and GaPE remarkably reduce the convergence time and improve the reconstruction quality by a large margin.

2 Related Work

3D Generation. Early methods on image-to-3D mainly employ Generative Adversarial Networks (GANs) to produce 3D representations, like point cloud [28], signed distance function (SDF) [51, 74, 3] or neural radiance field (NeRF) [12, 42]. By incorporating 2D GAN architectures [2, 8, 21, 23, 24, 25, 26, 73], 3D GANs have made remarkable advancements to generate 3D-aware content in a feed-forward manner. As a representative attempt, EG3D [3] employs GANs to generate samples in latent space and introduce a compact triplane representation for rendering novel views of 3D objects. Another research branch in 3D generation utilizes diffusion models (DMs) [59, 16, 46, 54, 44, 53, 17, 47], which have emerged with unprecedented success. One approach involves training 3D DMs directly using 3D supervision [14, 20, 41, 43, 52] or 2D supervision [1, 5, 13, 22, 36, 48]. However, these approaches suffer from 3D inconsistency and poor quality due to the lack of 3D priors. DreamFusion [45] introduces the Score Distillation Sampling (SDS) loss and generates NeRF under the supervision of pretrained large-scale 2D DMs. Variants of DreamFusion [6, 7, 15, 31, 32, 45, 50, 56, 61, 66] aim to reduce Janus (multi-faced) artifacts and improve geometry quality. However, the prolonged optimization process limits its practical application.

Sparse-view Reconstruction Multiview images provide stereo cues facilitating more accurate and detailed shape generation. Consequently, sparse view-based neural reconstruction methods [4, 19, 33, 39, 65, 70] achieve significant improvements in generalization to unseen scenes. However, challenges remain in capturing patterns within large-scale datasets. Scaling up the model and datasets is useful, but it also introduces new challenges, such as increased computational complexity. To address these challenges, recent methods leverage large-scale 3D datasets and well-designed multiview diffusion models (DMs) to generate multiple novel views from a single image [50, 62, 38, 37, 58, 57, 35, 49, 34, 30]. Subsequent steps involve neural reconstruction and Gaussian [27] or reconstruction [55, 69]. However, these explicit reconstruction methods face challenges due to multi-view inconsistency and low image resolution. Inspired by [18, 63, 74], we employ the recently proposed transformed-based large reconstruction model for implicit 3D shape generation.

Large Reconstruction Model The extensive 3D datasets [10, 9] have opened up new possibilities for training reconstruction models that can create 3D models from 2D images. LRM [18] first showcased the potential of using the transformer backbone to map image tokens to implicit 3D triplanes with multi-view supervision, resulting in highly generalizable models. Instant3D [29] achieves highly generalizable and high-quality single-image to 3D generation by extending LRM to a sparse-view reconstruction model and utilizing the prior in 2D diffusion models. While LGM [55] and GRM [69] models have replaced the triplane NeRF representation with 3D Gaussians [27] to improve

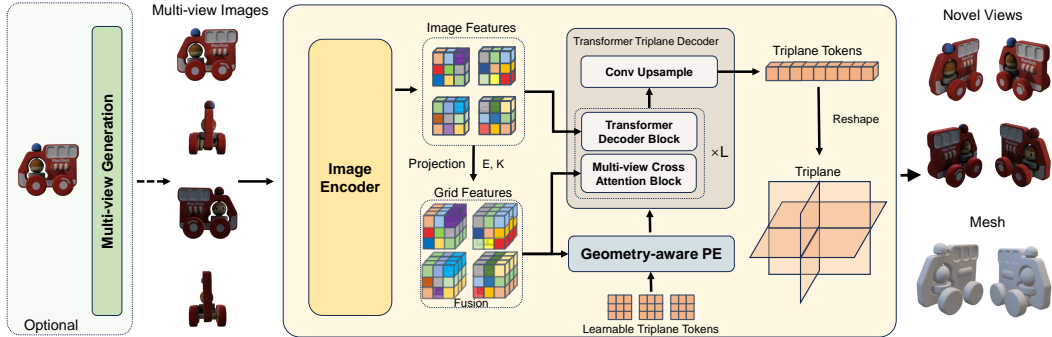


Figure 3: **Overview of M-LRM.** M-LRM is a fully differentiable transformer-based framework, featuring a feature encoder, geometry-aware position encoding and a multi-view cross attention block. Given multi-view images with corresponding camera poses, M-LRM incorporates the 2D and 3D features to efficiently conduct 3D-aware multi-view attention. The proposed geometry-aware position encoding allows more detailed and realistic 3D generation.

rendering efficiency, Gaussians have limitations in explicit geometry modeling and high-quality surface extraction. Concurrent works MVD² [72], CRM [67], and InstantMesh [68] use the same transformer backbone and focus on optimizing mesh representation for high-quality geometry and texture modeling. In contrast, our work focuses on incorporating 3D geometry prior to the memory-consuming transformer attention for efficient training. Moreover, our proposed M-LRM, featuring a novel 3D-aware transformer block, allows significant generalization in 3D shape modeling.

3 M-LRM

Fig. 3 illustrates the overall framework of our M-LRM. Unlike LRM which treats single-image-to-3D as a pure image translation problem, our method fully leverages the geometry prior to link 2D image and 3D triplane, thus achieving faster convergence and being able to generate results of better quality. Specifically, we achieve such advances in two steps. (1) Given multiple views of an object, we first extract the image features with an image encoder and propose *Geometry-aware Positional Embeddings* to initialize the learnable triplane tokens as detailed in Sec. 3.1. (2) With the learnable triplane tokens, we further adopt *Geometry-aware Cross Attention* to achieve the image feature injection in a geometry-aware manner as described in Sec. 3.2. Finally, we utilize the NeRF [40] renderer to generate 3D contents with the generated triplane token.

3.1 Geometry-aware Positional Embeddings

In LRM [18] and its variants [64, 29], the triplane tokens are randomly initialized without any priors and then optimized in the training. For convenience, we denote the randomly initialized triplane tokens as \mathbf{T}_r . In this section, we propose Geometry-aware Positional Embedding (GaPE) to better utilize image prior instead of the randomly initialized triplane tokens.

Geometry Volume Construction. Inspired by the previous multi-view reconstruction method [39], we aim to directly learn a geometry volume from the input images which encodes local geometric information based on the hints of multi-view consistency of the images. To cope with this, we first construct a grid volume whose vertices $\mathbf{X} = \{\mathbf{x}^j\}_{j \in \mathcal{J}}$ are uniformly sampled in the region of interest to be reconstructed. Considering the i -th view among the N input views, with its intrinsic $K_i \in \mathbb{R}^{3 \times 3}$ and extrinsic $E_i \in \mathbb{R}^{3 \times 4}$, we back project the vertices to the feature map of the i -th view F_i , and derive the corresponding feature grid $G_i = \{F_i(\pi_i(\mathbf{x}^j))\}_{j \in \mathcal{J}}$ for the i -th view, where π_i indicates the projection that projecting a 3D vertex onto the i -th image plane. The projection π_i is defined as

$$\tilde{\mathbf{u}}_i^j = \pi_i(\mathbf{x}^j) = K_i E_i \tilde{\mathbf{x}}^j, \quad (1)$$

where $\mathbf{x}^j \in \mathbb{R}^{3 \times 1}$ is the 3D coordinate of the grid vertex and $\tilde{\mathbf{x}}^j \in \mathbb{R}^{3 \times 1}$ is the homogeneous coordinate of \mathbf{x}^j . $\mathbf{u}_i^j \in \mathbb{R}^{2 \times 1}$ is the 2D coordinate of 2D image space and $\tilde{\mathbf{u}}_i^j \in \mathbb{R}^{3 \times 1}$ is the homogeneous coordinate of \mathbf{u}_i^j . With the obtained 2D coordinates, we could use `grid_sample` to extract corresponding features from the 2D feature map F_i . After back-projecting all the grid vertices, we obtain N feature grids $\{G_i\}_{i=1, \dots, N}$, which are fused together into one unified feature volume \mathbf{G} with a 3D convolution network.

Geometric Triplane Token. The feature volume \mathbf{G} contains the enriched prior produced by the image encoder. To introduce such prior to the triplane tokens, for each axis, we collect all the features of the volume along the axis, where the features of different vertices are concatenated, and obtain three feature maps $\mathbf{g}^{xy}, \mathbf{g}^{yz}, \mathbf{g}^{xz}$. The feature maps are further fed into three unique 2D convolutional networks to produce the positional embedding $\mathbf{T}_g^{xy}, \mathbf{T}_g^{yz}, \mathbf{T}_g^{xz}$. Finally, fusing the positional embedding and randomly initialized triplane tokens \mathbf{T}_r together yields the final geometry-aware triplane tokens as

$$\mathbf{T}_0 = \mathbf{T}_g + \mathbf{T}_r. \quad (2)$$

Since the tokens explicitly incorporate the geometric priors of the geometry volume, the tokens are geometry-aware and lead to faster convergence.

3.2 Efficient Geometry-aware Cross Attention

In addition to the geometry-aware triplane tokens, we introduce a novel cross-attention mechanism, named *Geometry-aware Cross Attention* (GCA), which incorporates explicit 3D-aware priors for enhanced information fusion between image features and triplane tokens. Specifically, unlike the vanilla attention used in previous LRM works [18, 64, 29] that accesses global features from all views, our method constructs an efficient attention mechanism. This mechanism ensures that each triplane token correlates with only a limited number of image feature tokens, improving computational efficiency and relevance.

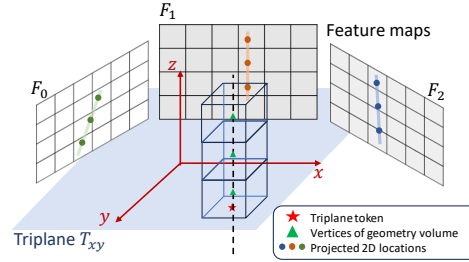


Figure 4: The illustration of Geometry-aware Cross Attention.

Our intuition is that each token in a triplane corresponds to a ray in the 3D space passing through the token, which can be projected into each view (as illustrated in Fig. 4). In other words, each token is related to a projected ray within a view rather than the entire view. Consequently, when performing cross-attention between each triplane token and the image features, we only need to correlate the triplane token with the feature tokens intersecting each projected ray. In prior works, dense cross-attention operates on $n \times h \times w$ feature tokens, where n is the number of views, and h and w are the height and width of the feature map. In contrast, our geometry-aware attention operates on only $n \times V$ feature tokens, where V is the size of the geometry volume. This significantly reduces the computational complexity and focuses attention on more relevant features.

The key to geometry-aware attention is extracting the feature tokens that intersect with each projected ray. By retaining the grid volume as mentioned, we can leverage Eq. 1 to project the relevant volume vertices into each view and obtain the corresponding 2D locations. Using these projected 2D locations, we can then access the related feature tokens for cross-attention. This approach ensures that the attention mechanism focuses on the most pertinent features, enhancing efficiency and relevance in the information fusion process.

Specifically, using a triplane token t^s as query, we implement the cross attention Attention $(Q, K, V) = \text{Softmax}\left(\frac{QK^T}{\sqrt{d}}\right) \cdot V$ with

$$Q = W^Q t^s, K = W^K [f_{e,l}^s]_{e \in \mathcal{E}, l \in \mathcal{L}}, V = W^V [f_{e,l}^s]_{e \in \mathcal{E}, l \in \mathcal{L}}, \quad (3)$$

where $[f_{e,l}^s]$ denote the features of the related projected feature tokens, W^Q , W^K and W^V are learnable matrices that project the inputs to query, key, and value, respectively.

To preserve global information interaction among different triplane tokens, we only replace half of the original transformer blocks with GCA, as it helps the model to preserve more details.

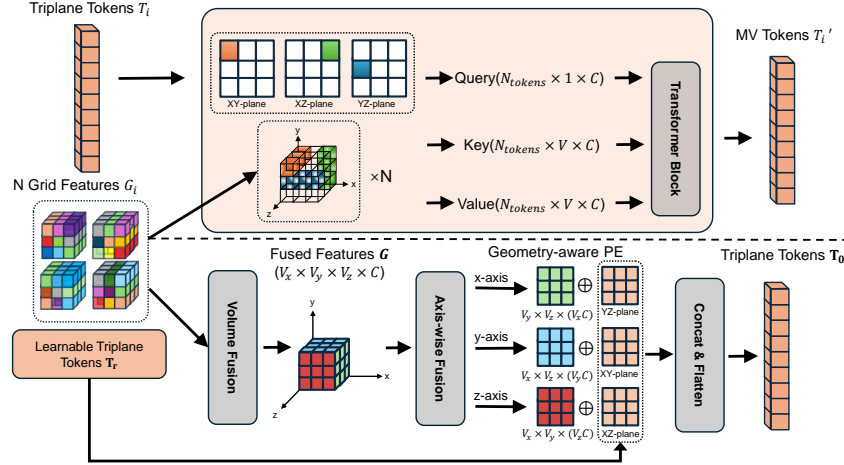


Figure 5: Illustration of Geometry-aware Cross Attention block (top) and Positional Embeddings (bottom).

3.3 Training Objectives

After we have the corresponding triplane P , we adopt differentiable NeRF renderer τ_N to render images and masks as $\{I^{pred}, m^{pred}\} = \tau_N(E, K|P)$. The predicted novel views are supervised via differentiable rendering by other sampled views. We adopt MSE loss, binary mask loss and LPIPS loss [71]. The training loss can be formulated as

$$\begin{aligned} \mathcal{L}_{\text{NeRF}} = & \lambda_{\text{mse}} \sum_i \left\| I_i^{\text{pred}} - I_i^{\text{gt}} \right\|_2 + \lambda_{\text{lips}} \sum_i \mathcal{L}_{\text{lips}} \left(I_i^{\text{pred}}, I_i^{\text{gt}} \right) \\ & + \lambda_{\text{mask}} \sum_i \left(m^{gt} \log m^{\text{pred}} + (1 - m^{gt}) \log (1 - m^{\text{pred}}) \right). \end{aligned} \quad (4)$$

4 Implementation Details and Datasets

Network Architecture. We train two variants of M-LRM, and here we provide details of our base variant. We refer to supplemental materials for more information on tiny variants.

For the image encoder, we utilize DINOv2-base with a patch size of 14. The transformer decoder consists of 12 layers with a hidden dimension of 768. We employ multi-head attention with 8 heads, and each head has a hidden dimension of 64. The learnable triplane tokens are initialized with a resolution of 64×64 and 768 channels. To upsample the triplane, we use a transpose convolution layer with a kernel size of 2 and a stride of 2, resulting in a resolution of 128×128 and 40 channels. The concatenated triplane features are then decoded using a 4-layer MLP into density and RGB values. We sample 192 points per ray.

We construct the spatial index volume and cost volume with a resolution of 64^3 . After projecting the image features into spatial volumes, we aggregate them using a 5-layer 3D convolution network with channel sizes of [64, 128, 128, 128, 64]. Additionally, we derive additional triplane features from the cost volume using three convolution layers with a kernel size of 3 and a stride of 1.

Other Implementation Details. M-LRM is trained on 32 NVIDIA H800 GPU (80GB) for 3 days. The batch size for each GPU was set to 1, and gradient accumulation was employed for 8 steps, resulting in a total batch size of 512. At each iteration, we randomly sample 10 views among the total 24 images, where 6 of them are used as input conditional images, and the other 4 for supervision. AdamW optimizer is used with β_1, β_2 set to 0.9, 0.95 respectively, and weight decay is set to 0.05. We increase the learning rate from $4e-10$ to $4e-4$ for the first epoch. After warmup, we adopt cosine annealing strategy for the learning rate and the learning rate decay drops to 0 at the end of training. The coefficients for different loss components are $\lambda_{\text{mse}} = 1.0$, $\lambda_{L1} = 0.2$, $\lambda_{\text{mask}} = 0.1$ and $\lambda_{\text{LPIPS}} = 1.0$. Following LGM [55], we adopt camera augmentation and image grid distortion as data augmentation.

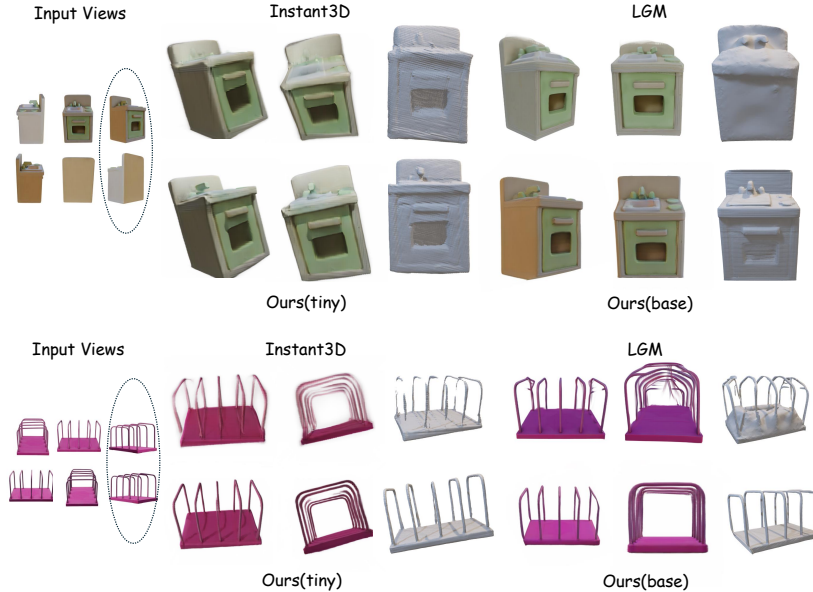


Figure 6: **Qualitative result of sparse-view reconstruction.** We compare our generated results with two baseline methods. Given the same input conditional views, our tiny model can generate results of higher fidelity and geometries that are more reasonable. Our base variant uses two additional views as input (the rightmost two images of the input views).

Dataset. We use the Objaverse dataset [10]. We filter out 190K objects among the 800K 3D models in the dataset. We use Blender to render 32 views per object. The 3D models are scaled to fit into the cubic bounding box, whose length is 1 and center is $(0, 0, 0)$. We set the field-of-view to 30° and the camera distance is calculated accordingly to ensure the object is well fitted at the center of the view. The first 8 views are sampled uniformly around the object with 0° elevation, the second 8 views are sampled uniformly with 20° elevation while the third 8 views are sampled with -20° elevation. The last 8 views are sampled randomly on the surface of the sphere. All cameras face towards $(0, 0, 0)$.

5 Experiments

5.1 Multi-view Reconstruction

Evaluation Setting. We compare our methods with Instant3D [29] and LGM [55] on Google Scanned Objects (GSO) [11]. Since the code and the model of Instant3D [29] are not available, we reproduce the model according to their paper. To fairly compare with Instant3D, we also train a tiny variant of our model that uses the same data as our reproduced Instant3D. We use the original implementation of LGM for the sparse view reconstruction task. Following existing work, we report PSNR, SSIM, and LPIPS to evaluate the visual quality of reconstruction and Chamfer distance (CD), F-Score(FS) for measuring the quality of the reconstructed mesh. We uniformly sample 16K points for measuring CD. We use two different threshold t to calculate FS for evaluation.

Results. As shown in Tab. 1, our proposed M-LRM outperforms all baselines by a large margin. Even though our Base version uses the most views compared to previous methods, our tiny version model still demonstrates the superiority of our proposed method. Compared to Instant3D, the tiny M-LRM converges much faster, and can generate images of higher fidelity. As for the LGM that uses the same number of input views, though our tiny model uses much less data than LGM, we can still generate images of higher quality, i.e. higher PSNR. However, the lack of data makes the model fail to generalize to the evaluation dataset, leading to higher LPIPS. Fig. 6 shows some visualization results of sparse-view reconstruction on the GSO dataset. Our method can not only generate novel views of better visual quality with no floaters, but also is able to extract meshes that are more plausible.



Figure 7: **Visualization result of single view to 3D generation.** We compare our method with Instant3D [29], LGM [55] and TripoSR [60]. The results of Instant3D suffer from blurry texture and severe geometry failure, while LGM [55] produces results with unreasonable color at the unseen region of the object. TripoSR can also generate visual results of high quality, but there remain many geometry artifacts. Our overall result is of better visual quality and geometry quality.

5.2 Single Image to 3D Generation

Evaluation Setting. For single image to 3D generation, we adopt Zero123++ [49] to generate multiple views as conditional images. For our tiny variant and our reproduced Instant3D that takes 4 views as input, we select the first, third, fifth, and sixth images generated by Zero123++. As our model is trained with white background, while zero123++ generates multi-view images with gray background, we opt to use a refined version of zero123++ [68] that generates multi-view images with white background. We compare our methods with Instant3D [29], LGM [55], and TripoSR [60]. For all methods, we render images at 512×512 resolution.

Table 1: Comparison with state-of-the-art image-to-3D counterparts on the Google Scanned Objects (GSO) dataset. \uparrow means the higher the better, and \downarrow indicates the lower the better.

| Method | # views | Train Res. | PSNR \uparrow | SSIM \uparrow | LPIPS \downarrow | CD \downarrow | FS (t=0.001) \downarrow | FS (t=0.01) \downarrow |
|--------------------|---------|------------|-----------------|-----------------|--------------------|-----------------|---------------------------|--------------------------|
| Instant3D [29] | 4 | 256 | 22.18 | 0.958 | 0.142 | 0.0069 | 0.3357 | 0.7739 |
| LGM [55] | 4 | 512 | 21.74 | 0.967 | 0.110 | 0.0034 | 0.7108 | 0.9273 |
| Ours (tiny) | 4 | 256 | 24.35 | 0.961 | 0.142 | 0.0068 | 0.3357 | 0.771 |
| Ours (Base) | 6 | 512 | 25.23 | 0.977 | 0.096 | 0.0011 | 0.8725 | 0.9695 |

Table 2: The ablation study of each component.

| GCA | GaPE | w/ Tr. Block | High Res. | PSNR \uparrow | SSIM \uparrow | LPIPS \downarrow |
|--------------|--------------|--------------|--------------|-----------------|-----------------|--------------------|
| \times | \times | \times | \times | 24.501 | 0.9746 | 0.1364 |
| \checkmark | \times | \times | \times | 24.923 | 0.9750 | 0.1322 |
| \times | \checkmark | \times | \times | 25.116 | 0.9765 | 0.1269 |
| \times | \times | \times | \checkmark | 26.219 | 0.9756 | 0.1201 |
| \checkmark | \checkmark | \checkmark | \times | 25.254 | 0.9772 | 0.1246 |
| \checkmark | \times | \checkmark | \checkmark | 26.966 | 0.9781 | 0.1067 |
| \checkmark | \checkmark | \checkmark | \checkmark | 27.581 | 0.9803 | 0.0986 |

Results. We compare the qualitative results of our generated results with those of baseline methods. As shown in Fig. 5, we use five examples to explain our qualitative experiment. The generation outcomes of Instant3D exhibit deficiencies in texture clarity and significant faults (Cases 2 and 4) in geometric representation (cases 2, 3). Similarly, the results produced by LGM [55] display unreasonable texture color in the unobserved regions of the object (cases 1, 4, 5). Besides, the meshes produced by LGM contain some geometry artifacts. This is because of the complex pipeline for extracting mesh from 3D Gaussian representation. Although TripoSR is capable of generating visually appealing results, it still exhibits numerous imperfections in geometric accuracy (cases 1, 5) due to the lack of explicit 3D spatial modeling. In contrast, as our proposed method is geometry-aware, it yields superior visual quality and improved geometric fidelity.

5.3 Ablation Study

We conduct ablation studies to demonstrate the effectiveness of our model components and architectural designs. We train these model variants with only Objaverse-LVIS subset. As shown in Tab. 2, GCA means using our proposed Multi-view Cross Attention module, GaPE means using Geometry-aware Positional Encoding, w/ Tr. Block means adding a transformer decoder block after our MCA block, and High Res. means using 64 as the resolution of the initial triplane and the geometry volume, as opposed to the original 32. When High Res. is adopted, we sample 192 points per ray in volumetric rendering instead of 96 originally.

The results of the first two rows and the last two rows demonstrate the effectiveness of our proposed GCA and GaPE. As shown in the table, adding a transformer decoder block after GCA block improves the model’s performance, indicating that preserving global attention is helpful. We also show that using High Res. setting can enhance the model’s capability by a large margin.

6 Conclusion and Limitation

Conclusion. In this work, we introduce the Multi-view Large Reconstruction Model (M-LRM), which is designed to efficiently reconstruct high-quality 3D shapes from multiple views in a 3D-aware manner. Our proposed approach incorporates a multi-view consistent cross-attention scheme, enabling M-LRM to accurately extract relevant information from the input images. Additionally, we leverage the 3D priors of the input multi-view images to initialize the tri-plane tokens. By doing so, our model surpasses the capabilities of instant3D and produces 3D shapes with exceptional fidelity. Experimental results demonstrate that our model substantially improves performance and exhibits faster training convergence compared to instant3D and other LRM-series work.

Limitations and Future Work. However, we notice that there are still some limitations in our framework. (i) Currently, our model can only accept a fixed number of views as input. However, our model can be further extended to support arbitrary input views, which will be left as future work.

(ii) Although our model is trained with augmented data, its performance would still inevitably be affected by inconsistent multi-view input when doing single-view to 3D generation tasks. However, we believe that this problem can be solved as the multi-view generation models advance.

References

- [1] Titas Anciukevičius, Zexiang Xu, Matthew Fisher, Paul Henderson, Hakan Bilen, Niloy J Mitra, and Paul Guerrero. Renderdiffusion: Image diffusion for 3d reconstruction, inpainting and generation. In *Proceedings of the IEEE/CVF Conference on Computer Vision and Pattern Recognition*, pages 12608–12618, 2023.
- [2] Andrew Brock, Jeff Donahue, and Karen Simonyan. Large scale gan training for high fidelity natural image synthesis. *arXiv preprint arXiv:1809.11096*, 2018.
- [3] Eric R Chan, Connor Z Lin, Matthew A Chan, Koki Nagano, Boxiao Pan, Shalini De Mello, Orazio Gallo, Leonidas J Guibas, Jonathan Tremblay, Sameh Khamis, et al. Efficient geometry-aware 3d generative adversarial networks. In *Proceedings of the IEEE/CVF conference on computer vision and pattern recognition*, pages 16123–16133, 2022.
- [4] Anpei Chen, Zexiang Xu, Fuqiang Zhao, Xiaoshuai Zhang, Fanbo Xiang, Jingyi Yu, and Hao Su. Mvsnerf: Fast generalizable radiance field reconstruction from multi-view stereo. In *Proceedings of the IEEE/CVF international conference on computer vision*, pages 14124–14133, 2021.
- [5] Hansheng Chen, Jiatao Gu, Anpei Chen, Wei Tian, Zhuowen Tu, Lingjie Liu, and Hao Su. Single-stage diffusion nerf: A unified approach to 3d generation and reconstruction. In *Proceedings of the IEEE/CVF International Conference on Computer Vision*, pages 2416–2425, 2023.
- [6] Rui Chen, Yongwei Chen, Ningxin Jiao, and Kui Jia. Fantasia3d: Disentangling geometry and appearance for high-quality text-to-3d content creation. In *Proceedings of the IEEE/CVF International Conference on Computer Vision*, pages 22246–22256, 2023.
- [7] Jaeyoung Chung, Suyoung Lee, Hyeongjin Nam, Jaerin Lee, and Kyoung Mu Lee. Luciddreamer: Domain-free generation of 3d gaussian splatting scenes. *arXiv preprint arXiv:2311.13384*, 2023.
- [8] Antonia Creswell, Tom White, Vincent Dumoulin, Kai Arulkumaran, Biswa Sengupta, and Anil A Bharath. Generative adversarial networks: An overview. *IEEE signal processing magazine*, 35(1):53–65, 2018.
- [9] Matt Deitke, Ruoshi Liu, Matthew Wallingford, Huong Ngo, Oscar Michel, Aditya Kusupati, Alan Fan, Christian Laforte, Vikram Voleti, Samir Yitzhak Gadre, et al. Objaverse-xl: A universe of 10m+ 3d objects. *Advances in Neural Information Processing Systems*, 36, 2024.
- [10] Matt Deitke, Dustin Schwenk, Jordi Salvador, Luca Weihs, Oscar Michel, Eli VanderBilt, Ludwig Schmidt, Kiana Ehsani, Aniruddha Kembhavi, and Ali Farhadi. Objaverse: A universe of annotated 3d objects. In *Proceedings of the IEEE/CVF Conference on Computer Vision and Pattern Recognition*, pages 13142–13153, 2023.
- [11] Laura Downs, Anthony Francis, Nate Koenig, Brandon Kinman, Ryan Hickman, Krista Reymann, Thomas B McHugh, and Vincent Vanhoucke. Google scanned objects: A high-quality dataset of 3d scanned household items. In *2022 International Conference on Robotics and Automation (ICRA)*, pages 2553–2560. IEEE, 2022.
- [12] Jiatao Gu, Lingjie Liu, Peng Wang, and Christian Theobalt. Stylenerf: A style-based 3d-aware generator for high-resolution image synthesis. *arXiv preprint arXiv:2110.08985*, 2021.
- [13] Jiatao Gu, Alex Trevithick, Kai-En Lin, Joshua M Susskind, Christian Theobalt, Lingjie Liu, and Ravi Ramamoorthi. Nerfdiff: Single-image view synthesis with nerf-guided distillation from 3d-aware diffusion. In *International Conference on Machine Learning*, pages 11808–11826. PMLR, 2023.
- [14] Anchit Gupta, Wenhan Xiong, Yixin Nie, Ian Jones, and Barlas Oğuz. 3dgen: Triplane latent diffusion for textured mesh generation. *arXiv preprint arXiv:2303.05371*, 2023.
- [15] Amir Hertz, Kfir Aberman, and Daniel Cohen-Or. Delta denoising score. In *Proceedings of the IEEE/CVF International Conference on Computer Vision*, pages 2328–2337, 2023.

- [16] Jonathan Ho, Ajay Jain, and Pieter Abbeel. Denoising diffusion probabilistic models. *Advances in neural information processing systems*, 33:6840–6851, 2020.
- [17] Jonathan Ho, Ajay Jain, and Pieter Abbeel. Denoising diffusion probabilistic models. 2020.
- [18] Yicong Hong, Kai Zhang, Jiuxiang Gu, Sai Bi, Yang Zhou, Difan Liu, Feng Liu, Kalyan Sunkavalli, Trung Bui, and Hao Tan. Lrm: Large reconstruction model for single image to 3d. *arXiv preprint arXiv:2311.04400*, 2023.
- [19] Ajay Jain, Matthew Tancik, and Pieter Abbeel. Putting nerf on a diet: Semantically consistent few-shot view synthesis. In *Proceedings of the IEEE/CVF International Conference on Computer Vision*, pages 5885–5894, 2021.
- [20] Heewoo Jun and Alex Nichol. Shap-e: Generating conditional 3d implicit functions. *arXiv preprint arXiv:2305.02463*, 2023.
- [21] Minguk Kang, Jun-Yan Zhu, Richard Zhang, Jaesik Park, Eli Shechtman, Sylvain Paris, and Taesung Park. Scaling up gans for text-to-image synthesis. In *Proceedings of the IEEE/CVF Conference on Computer Vision and Pattern Recognition*, pages 10124–10134, 2023.
- [22] Animesh Karnewar, Andrea Vedaldi, David Novotny, and Niloy J Mitra. Holodiffusion: Training a 3d diffusion model using 2d images. In *Proceedings of the IEEE/CVF conference on computer vision and pattern recognition*, pages 18423–18433, 2023.
- [23] Tero Karras, Timo Aila, Samuli Laine, and Jaakko Lehtinen. Progressive growing of gans for improved quality, stability, and variation. *arXiv preprint arXiv:1710.10196*, 2017.
- [24] Tero Karras, Miika Aittala, Samuli Laine, Erik Härkönen, Janne Hellsten, Jaakko Lehtinen, and Timo Aila. Alias-free generative adversarial networks. *Advances in neural information processing systems*, 34:852–863, 2021.
- [25] Tero Karras, Samuli Laine, and Timo Aila. A style-based generator architecture for generative adversarial networks. In *Proceedings of the IEEE/CVF conference on computer vision and pattern recognition*, pages 4401–4410, 2019.
- [26] Tero Karras, Samuli Laine, Miika Aittala, Janne Hellsten, Jaakko Lehtinen, and Timo Aila. Analyzing and improving the image quality of stylegan. In *Proceedings of the IEEE/CVF conference on computer vision and pattern recognition*, pages 8110–8119, 2020.
- [27] Bernhard Kerbl, Georgios Kopanas, Thomas Leimkühler, and George Drettakis. 3d gaussian splatting for real-time radiance field rendering. *ACM Transactions on Graphics*, 42(4):1–14, 2023.
- [28] Chun-Liang Li, Manzil Zaheer, Yang Zhang, Barnabas Póczos, and Ruslan Salakhutdinov. Point cloud gan. *arXiv preprint arXiv:1810.05795*, 2018.
- [29] Jiahao Li, Hao Tan, Kai Zhang, Zexiang Xu, Fujun Luan, Yinghao Xu, Yicong Hong, Kalyan Sunkavalli, Greg Shakhnarovich, and Sai Bi. Instant3d: Fast text-to-3d with sparse-view generation and large reconstruction model. *arXiv preprint arXiv:2311.06214*, 2023.
- [30] Peng Li, Yuan Liu, Xiaoxiao Long, Feihu Zhang, Cheng Lin, Mengfei Li, Xingqun Qi, Shanghang Zhang, Wenhan Luo, Ping Tan, et al. Era3d: High-resolution multiview diffusion using efficient row-wise attention. *arXiv preprint arXiv:2405.11616*, 2024.
- [31] Yixun Liang, Xin Yang, Jiantao Lin, Haodong Li, Xiaogang Xu, and Yingcong Chen. Lucidreamer: Towards high-fidelity text-to-3d generation via interval score matching. *arXiv preprint arXiv:2311.11284*, 2023.
- [32] Chen-Hsuan Lin, Jun Gao, Luming Tang, Towaki Takikawa, Xiaohui Zeng, Xun Huang, Karsten Kreis, Sanja Fidler, Ming-Yu Liu, and Tsung-Yi Lin. Magic3d: High-resolution text-to-3d content creation. In *Proceedings of the IEEE/CVF Conference on Computer Vision and Pattern Recognition*, pages 300–309, 2023.
- [33] Kai-En Lin, Yen-Chen Lin, Wei-Sheng Lai, Tsung-Yi Lin, Yi-Chang Shih, and Ravi Ramamoorthi. Vision transformer for nerf-based view synthesis from a single input image. In *Proceedings of the IEEE/CVF Winter Conference on Applications of Computer Vision*, pages 806–815, 2023.
- [34] Minghua Liu, Chao Xu, Haian Jin, Linghao Chen, Mukund Varma T, Zexiang Xu, and Hao Su. One-2-3-45: Any single image to 3d mesh in 45 seconds without per-shape optimization, 2023.
- [35] Ruoshi Liu, Rundi Wu, Basile Van Hoorick, Pavel Tokmakov, Sergey Zakharov, and Carl Vondrick. Zero-1-to-3: Zero-shot one image to 3d object, 2023.

- [36] Ruoshi Liu, Rundi Wu, Basile Van Hoorick, Pavel Tokmakov, Sergey Zakharov, and Carl Vondrick. Zero-1-to-3: Zero-shot one image to 3d object. In *Proceedings of the IEEE/CVF International Conference on Computer Vision*, pages 9298–9309, 2023.
- [37] Yuan Liu, Cheng Lin, Zijiao Zeng, Xiaoxiao Long, Lingjie Liu, Taku Komura, and Wenping Wang. Syncdreamer: Generating multiview-consistent images from a single-view image. *arXiv preprint arXiv:2309.03453*, 2023.
- [38] Xiaoxiao Long, Yuan-Chen Guo, Cheng Lin, Yuan Liu, Zhiyang Dou, Lingjie Liu, Yuexin Ma, Song-Hai Zhang, Marc Habermann, Christian Theobalt, et al. Wonder3d: Single image to 3d using cross-domain diffusion. *arXiv preprint arXiv:2310.15008*, 2023.
- [39] Xiaoxiao Long, Cheng Lin, Peng Wang, Taku Komura, and Wenping Wang. Sparseneus: Fast generalizable neural surface reconstruction from sparse views. In *European Conference on Computer Vision*, pages 210–227. Springer, 2022.
- [40] Ben Mildenhall, Pratul P Srinivasan, Matthew Tancik, Jonathan T Barron, Ravi Ramamoorthi, and Ren Ng. Nerf: Representing scenes as neural radiance fields for view synthesis. *Communications of the ACM*, 65(1):99–106, 2021.
- [41] Alex Nichol, Heewoo Jun, Prafulla Dhariwal, Pamela Mishkin, and Mark Chen. Point-e: A system for generating 3d point clouds from complex prompts. *arXiv preprint arXiv:2212.08751*, 2022.
- [42] Michael Niemeyer and Andreas Geiger. Giraffe: Representing scenes as compositional generative neural feature fields. In *Proceedings of the IEEE/CVF Conference on Computer Vision and Pattern Recognition*, pages 11453–11464, 2021.
- [43] Evangelos Ntavelis, Aliaksandr Siarohin, Kyle Olszewski, Chaoyang Wang, Luc V Gool, and Sergey Tulyakov. Autodecoding latent 3d diffusion models. *Advances in Neural Information Processing Systems*, 36:67021–67047, 2023.
- [44] Ryan Po, Wang Yifan, Vladislav Golyanik, Kfir Aberman, Jonathan T Barron, Amit H Bermano, Eric Ryan Chan, Tali Dekel, Aleksander Holynski, Angjoo Kanazawa, et al. State of the art on diffusion models for visual computing. *arXiv preprint arXiv:2310.07204*, 2023.
- [45] Ben Poole, Ajay Jain, Jonathan T Barron, and Ben Mildenhall. Dreamfusion: Text-to-3d using 2d diffusion. *arXiv preprint arXiv:2209.14988*, 2022.
- [46] Robin Rombach, Andreas Blattmann, Dominik Lorenz, Patrick Esser, and Björn Ommer. High-resolution image synthesis with latent diffusion models. In *Proceedings of the IEEE/CVF conference on computer vision and pattern recognition*, pages 10684–10695, 2022.
- [47] Robin Rombach, Andreas Blattmann, Dominik Lorenz, Patrick Esser, and Björn Ommer. High-resolution image synthesis with latent diffusion models. 2022.
- [48] Bokui Shen, Xinchun Yan, Charles R Qi, Mahyar Najibi, Boyang Deng, Leonidas Guibas, Yin Zhou, and Dragomir Anguelov. Gina-3d: Learning to generate implicit neural assets in the wild. In *Proceedings of the IEEE/CVF conference on computer vision and pattern recognition*, pages 4913–4926, 2023.
- [49] Ruoxi Shi, Hansheng Chen, Zhuoyang Zhang, Minghua Liu, Chao Xu, Xinyue Wei, Linghao Chen, Chong Zeng, and Hao Su. Zero123++: a single image to consistent multi-view diffusion base model. *arXiv preprint arXiv:2310.15110*, 2023.
- [50] Yichun Shi, Peng Wang, Jianglong Ye, Mai Long, Kejie Li, and Xiao Yang. Mvdream: Multi-view diffusion for 3d generation. *arXiv preprint arXiv:2308.16512*, 2023.
- [51] Zifan Shi, Sida Peng, Yinghao Xu, Andreas Geiger, Yiyi Liao, and Yujun Shen. Deep generative models on 3d representations: A survey. *arXiv preprint arXiv:2210.15663*, 2022.
- [52] J Ryan Shue, Eric Ryan Chan, Ryan Po, Zachary Ankner, Jiajun Wu, and Gordon Wetzstein. 3d neural field generation using triplane diffusion. In *Proceedings of the IEEE/CVF Conference on Computer Vision and Pattern Recognition*, pages 20875–20886, 2023.
- [53] Jiaming Song, Chenlin Meng, and Stefano Ermon. Denoising diffusion implicit models. *arXiv preprint arXiv:2010.02502*, 2020.
- [54] Yang Song, Jascha Sohl-Dickstein, Diederik P Kingma, Abhishek Kumar, Stefano Ermon, and Ben Poole. Score-based generative modeling through stochastic differential equations. *arXiv preprint arXiv:2011.13456*, 2020.

- [55] Jiaxiang Tang, Zhaoxi Chen, Xiaokang Chen, Tengfei Wang, Gang Zeng, and Ziwei Liu. Lgm: Large multi-view gaussian model for high-resolution 3d content creation, 2024.
- [56] Jiaxiang Tang, Jiawei Ren, Hang Zhou, Ziwei Liu, and Gang Zeng. Dreamgaussian: Generative gaussian splatting for efficient 3d content creation. *arXiv preprint arXiv:2309.16653*, 2023.
- [57] Shitao Tang, Jiacheng Chen, Dilin Wang, Chengzhou Tang, Fuyang Zhang, Yuchen Fan, Vikas Chandra, Yasutaka Furukawa, and Rakesh Ranjan. Mvdifffusion++: A dense high-resolution multi-view diffusion model for single or sparse-view 3d object reconstruction. *arXiv preprint arXiv:2402.12712*, 2024.
- [58] Shitao Tang, Fuayng Zhang, Jiacheng Chen, Peng Wang, and Furukawa Yasutaka. Mvdifffusion: Enabling holistic multi-view image generation with correspondence-aware diffusion. *arXiv preprint 2307.01097*, 2023.
- [59] Ayush Tewari, Tianwei Yin, George Cazenavette, Semon Rezhikov, Josh Tenenbaum, Frédo Durand, Bill Freeman, and Vincent Sitzmann. Diffusion with forward models: Solving stochastic inverse problems without direct supervision. *Advances in Neural Information Processing Systems*, 36, 2024.
- [60] Dmitry Tochilkin, David Pankratz, Zexiang Liu, Zixuan Huang, , Adam Letts, Yangguang Li, Ding Liang, Christian Laforte, Varun Jampani, and Yan-Pei Cao. Triposr: Fast 3d object reconstruction from a single image. *arXiv preprint arXiv:2403.02151*, 2024.
- [61] Haochen Wang, Xiaodan Du, Jiahao Li, Raymond A Yeh, and Greg Shakhnarovich. Score jacobian chaining: Lifting pretrained 2d diffusion models for 3d generation. In *Proceedings of the IEEE/CVF Conference on Computer Vision and Pattern Recognition*, pages 12619–12629, 2023.
- [62] Peng Wang and Yichun Shi. Imagedream: Image-prompt multi-view diffusion for 3d generation. *arXiv preprint arXiv:2312.02201*, 2023.
- [63] Peng Wang, Hao Tan, Sai Bi, Yinghao Xu, Fujun Luan, Kalyan Sunkavalli, Wenping Wang, Zexiang Xu, and Kai Zhang. Pf-lrm: Pose-free large reconstruction model for joint pose and shape prediction. *arXiv preprint arXiv:2311.12024*, 2023.
- [64] Peng Wang, Hao Tan, Sai Bi, Yinghao Xu, Fujun Luan, Kalyan Sunkavalli, Wenping Wang, Zexiang Xu, and Kai Zhang. Pf-lrm: Pose-free large reconstruction model for joint pose and shape prediction. *arXiv preprint arXiv:2311.12024*, 2023.
- [65] Qianqian Wang, Zhicheng Wang, Kyle Genova, Pratul P Srinivasan, Howard Zhou, Jonathan T Barron, Ricardo Martin-Brualla, Noah Snavely, and Thomas Funkhouser. Ibrnet: Learning multi-view image-based rendering. In *Proceedings of the IEEE/CVF Conference on Computer Vision and Pattern Recognition*, pages 4690–4699, 2021.
- [66] Zhengyi Wang, Cheng Lu, Yikai Wang, Fan Bao, Chongxuan Li, Hang Su, and Jun Zhu. Pro-lificdreamer: High-fidelity and diverse text-to-3d generation with variational score distillation. *Advances in Neural Information Processing Systems*, 36, 2024.
- [67] Zhengyi Wang, Yikai Wang, Yifei Chen, Chendong Xiang, Shuo Chen, Dajiang Yu, Chongxuan Li, Hang Su, and Jun Zhu. Crm: Single image to 3d textured mesh with convolutional reconstruction model. *arXiv preprint arXiv:2403.05034*, 2024.
- [68] Jiale Xu, Weihao Cheng, Yiming Gao, Xintao Wang, Shenghua Gao, and Ying Shan. Instantmesh: Efficient 3d mesh generation from a single image with sparse-view large reconstruction models. *arXiv preprint arXiv:2404.07191*, 2024.
- [69] Yinghao Xu, Zifan Shi, Wang Yifan, Hansheng Chen, Ceyuan Yang, Sida Peng, Yujun Shen, and Gordon Wetzstein. Grm: Large gaussian reconstruction model for efficient 3d reconstruction and generation. *arXiv preprint arXiv:2403.14621*, 2024.
- [70] Alex Yu, Vickie Ye, Matthew Tancik, and Angjoo Kanazawa. pixelnerf: Neural radiance fields from one or few images. In *Proceedings of the IEEE/CVF Conference on Computer Vision and Pattern Recognition*, pages 4578–4587, 2021.
- [71] Richard Zhang, Phillip Isola, Alexei A Efros, Eli Shechtman, and Oliver Wang. The unreasonable effectiveness of deep features as a perceptual metric. In *Proceedings of the IEEE conference on computer vision and pattern recognition*, pages 586–595, 2018.
- [72] Xin-Yang Zheng, Hao Pan, Yu-Xiao Guo, Xin Tong, and Yang Liu. Mvd²: Efficient multiview 3d reconstruction for multiview diffusion, 2024.

- [73] Jiapeng Zhu, Ceyuan Yang, Kecheng Zheng, Yinghao Xu, Zifan Shi, and Yujun Shen. Exploring sparse moe in gans for text-conditioned image synthesis. *arXiv preprint arXiv:2309.03904*, 2023.
- [74] Zi-Xin Zou, Zhipeng Yu, Yuan-Chen Guo, Yangguang Li, Ding Liang, Yan-Pei Cao, and Song-Hai Zhang. Triplane meets gaussian splatting: Fast and generalizable single-view 3d reconstruction with transformers. *arXiv preprint arXiv:2312.09147*, 2023.